Real-time lineage analysis reveals oriented cell divisions associated with morphogenesis at the shoot apex of *Arabidopsis thaliana*

G. Venugopala Reddy[1], Marcus G. Heisler[1], David W. Ehrhardt[2] and Elliot M. Meyerowitz[1,*]

[1]California Institute of Technology, Division of Biology, MC 156-29, 1200 E. California Boulevard, Pasadena, CA 91125, USA
[2]Department of Plant Biology, Carnegie Institution of Washington, Stanford, CA 94305, USA
*Author for correspondence (e-mail: meyerow@its.caltech.edu)

Accepted 11 May 2004

Development 131, 4225-4237
Published by The Company of Biologists 2004
doi:10.1242/dev.01261

Summary

Precise knowledge of spatial and temporal patterns of cell division, including number and orientation of divisions, and knowledge of cell expansion, is central to understanding morphogenesis. Our current knowledge of cell division patterns during plant and animal morphogenesis is largely deduced from analysis of clonal shapes and sizes. But such an analysis can reveal only the number, not the orientation or exact rate, of cell divisions. In this study, we have analyzed growth in real time by monitoring individual cell divisions in the shoot apical meristems (SAMs) of *Arabidopsis thaliana*. The live imaging technique has led to the development of a spatial and temporal map of cell division patterns. We have integrated cell behavior over time to visualize growth. Our analysis reveals temporal variation in mitotic activity and the cell division is coordinated across clonally distinct layers of cells. Temporal variation in mitotic activity is not correlated to the estimated plastochron length and diurnal rhythms. Cell division rates vary across the SAM surface. Cells in the peripheral zone (PZ) divide at a faster rate than in the central zone (CZ). Cell division rates in the CZ are relatively heterogeneous when compared with PZ cells. We have analyzed the cell behavior associated with flower primordium development starting from a stage at which the future flower comprises four cells in the L1 epidermal layer. Primordium development is a sequential process linked to distinct cellular behavior. Oriented cell divisions, in primordial progenitors and in cells located proximal to them, are associated with initial primordial outgrowth. The oriented cell divisions are followed by a rapid burst of cell expansion and cell division, which transforms a flower primordium into a three-dimensional flower bud. Distinct lack of cell expansion is seen in a narrow band of cells, which forms the boundary region between developing flower bud and the SAM. We discuss these results in the context of SAM morphogenesis.

Movies available online

Key words: Live imaging, Lineage analysis, Shoot apical meristem

Introduction

One of the challenges in both animal and plant developmental biology is to understand the cellular basis of pattern formation. Detailed understanding of the dynamic patterns of cell division, both of number of divisions and their orientation in a developing field is central to understanding morphogenesis (Meyerowitz, 1997). It has become clear over the years that the task of recording a dynamic spatio-temporal pattern of cell behavior is not trivial (Steeves and Sussex, 1989). Morphogenetic studies on the wing disc of *Drosophila* and lateral organs in plants have employed lineage analysis and subsequent comparison of clonal shapes and sizes to infer cell behavior (Dolan and Poethig, 1998; Gonzalez-Gaitan et al., 1994; Resino et al., 2002). A recent study on *Antirrhinum* petal lobe development has utilized inferred cell behavior from clonal analysis to generate growth models (Rolland-Lagan et al., 2003). But the direct experimental determination of cell behavior, in real time and in a morphogenetic context is generally lacking in both animals and plants.

The shoot apical meristem (SAM) of *Arabidopsis thaliana* presents an elegant system for the study of cell behavior in a morphogenetic context. The essential function of the SAM is to produce the cells that comprise the aboveground plant parts. The SAM is a multilayered structure consisting of three clonally distinct layers of cells. The outermost L1 and the sub-epidermal L2 are single layers in which anticlinal divisions occur, while the underlying corpus forms a multilayered structure with cell division in periclinal as well as anticlinal planes (Steeves and Sussex, 1989). Within this framework, the SAM can be divided into cytological zones, where the central zone (CZ) is at the very apex, the peripheral zone (PZ) is on the sides, and the rib meristem (RM) is in the central part of the meristem. The CZ has been thought to harbor a set of initials, which divide and displace their daughters into the PZ, where they are incorporated into the primordia of leaves and flowers at defined locations. Starting just after germination, the first four leaves are formed as opposite pairs, and then subsequent leaves and flowers are formed in a spiral pattern with an angle close to 137.5° between consecutive primordia (Callos et al., 1994). The SAM retains a nearly constant size from germination to senescence, despite a constant flux of cells from the meristem to newly established lateral organs and underlying stem. Thus the SAM has to coordinate two independent but related functions, first to ensure a constant cell

number in different regions of the SAM, and at the same time to allow cells in defined locations to differentiate and become part of primordia. A tight coordination between cell division and displacement of the progeny, both within and across clonally distinct layers of the SAM, has been proposed to be a major factor in regulating the size of the SAM and in generating the radial pattern of the shoot apex (Meyerowitz, 1997). In plants, such a coordination must be achieved predominantly through controlled patterns of cell division and expansion, as common animal mechanisms such as programmed cell death and cell migration do not operate during SAM morphogenesis.

Genetic studies have revealed signaling mechanisms involved in meristem maintenance. Mutations in *CLAVATA (CLV)* genes (*CLV1*, *CLV2* and *CLV3*) result in larger meristems, while mutations in *WUSCHEL (WUS)* result in a failure to maintain a functional meristem (Clark et al., 1993; Clark et al., 1995; Laux et al., 1996; Kayes and Clark, 1998). Several studies have contributed to a model involving positive and negative feedback loops to maintain meristem size (Clark et al., 1997; Mayer et al., 1998; Fletcher et al., 1999; Brand et al., 2000; Schoof et al., 2000). The function of WUS, a homeodomain transcription factor, is required to maintain a constant stem-cell pool in the CZ and at the same time CLV1, a receptor kinase, and CLV3, a small secreted protein, function to repress WUS activity. The function of SHOOT MERISTEMLESS (STM) adds another layer of regulation in SAM establishment and/or maintenance (Long et al., 1996). *stm* mutants fail to develop a functional SAM, and STM has been proposed to function in maintenance of cell proliferation by repressing genes such as *ASYMMETRIC LEAVES1 (AS1)*, which are specific to developing leaves at the periphery (Byrne et al., 2000). Auxin distribution has been shown to mediate the placement of primordia within the PZ (Reinhardt et al., 2003b). These studies demonstrate a role for short-range signaling between adjacent groups of cells, both within and across clonally distinct layers of cells. Understanding how these signaling mechanisms interface with cell division patterns is central to understanding meristem maintenance and morphogenesis.

Our knowledge of cell division patterns in SAMs is limited, though it has been a subject of intense analytical investigation since early in the last century (Steeves and Sussex, 1989; Meyerowitz, 1997). Early studies based on cytological appearance and also on counts of mitotic figures in different regions of the SAM have reached a broad consensus that cells in the CZ divide more slowly than cells in the PZ. Efforts have also been made to record cell behavior in living shoot apices (Ball, 1960; Soma and Ball, 1964). These studies did reveal cell displacement patterns but visualized only epidermal cells. The studies on the surface expansion of the SAMs have yielded quantitative description of cell expansion behavior (Hernandez et al., 1991; Dumais and Kwiatkowska, 2002; Kwiatkowska and Dumais, 2003; Kwiatkowska, 2004). A comprehensive morphometric analysis in *Arabidopsis thaliana* has revealed spatial patterns of mitotic activity in different regions of the SAMs (Laufs et al., 1998). A recent in-vivo study in *Arabidopsis thaliana*, based on optical imaging, has revealed the effects of anti-mitotic drugs and DNA synthesis inhibitors on differentiation and morphogenesis at the shoot apex (Grandjean et al., 2003). Sector boundary analysis has predicted the number of initial cells for both the leaf and flower formation (Irish and Sussex, 1992; Bossinger and Smyth, 1996). Although all these studies have yielded insights at several levels, a comprehensive dynamic view of cell behavior is lacking.

In this study we have analyzed cell division patterns in living and actively growing wild-type SAMs of *Arabidopsis thaliana*. One of the major challenges in observing cells in living SAMs has been the accessibility of these cells, as they are shrouded by developing primordia. We have designed a live-imaging technique based on confocal microscopy and have employed a variety of cell division and cell structure markers to observe cell division and cell expansion in real time. We have used the time-lapse imaging data to reconstruct events in time by utilizing image registration algorithms to visualize morphogenesis in relation to cell behavior. Finally, we have incorporated time-lapse data to serially reconstruct lineages in real time. Our analysis reveals that distinct cell behavior is associated with different stages of primordium morphogenesis. We show that the amount of cell division is comparable across successive primordial regions. Oriented cell divisions, in primordial progenitors and in cells located proximal to them, is associated with initial primordial outgrowth, followed by a rapid and coordinated burst of cell expansion and cell division to transform this extension into a three-dimensional flower bud. This study provides a dynamic spatio-temporal analysis of cell division in SAMs that can form a basis for future quantitative studies of meristematic cell behavior.

Materials and methods

Transgenic lines and growth conditions

The plasmids harboring plasma membrane marker 35S::YFP29-1 and 35S::H2B:mYFP (gift from Jim Haseloff, University of Cambridge) were introduced into the Landsberg *erecta* ecotype by the floral dip method (Clough and Bent, 1998). Primary transformants were selected and screened for uniform and strong expression. Homozygous plants showed brighter fluorescence than heterozygous plants and were more suitable for time-lapse imaging. In the case of 35S::H2B:mYFP, the homozygous insertion line grew poorly compared with heterozygous siblings. Heterozygous plants were therefore used for time-lapse imaging. The cyclinB1;1:GFP (BJ3) construct is in the Columbia ecotype and was generated by replacing the β-glucuronidase coding region in the original construct described earlier (Colon-Cormona et al., 1997) with a GFP-coding region (Peter Doerner, personal communication). All plants grown either on soil or on plates were maintained in continuous light and at 18-20°C.

Live imaging

Plants were germinated on MS-agar plates and allowed to grow for 10 days before they were transferred into clear plastic boxes containing MS-agar. The plants were maintained in aseptic conditions until bolting. Upon bolting, when the shoot apex emerged out of the rosette, the plants were prepared for time-lapse imaging. The MS-agar surface was overlaid with 1% agarose to minimize contamination. The older floral buds were carefully removed or spaced out in order to expose the SAM. The rosette was stabilized by applying 1.5% molten agarose onto the stem. FM4-64 (50 μg/ml), when used, was applied directly onto the SAM 30 minutes prior to imaging.

Microscopy and image processing

Plants were imaged by using a Zeiss 310 or Zeiss 510 upright confocal microscope using a 63× water dipping achroplan lens, which has a working distance of 2 mm. Plastic boxes were filled with water to

submerge the plant prior to each imaging session, which lasted for 30 seconds to 1 minute. The water was then discarded and the plants were returned to normal growth conditions. This process was repeated for imaging intervals as described for individual experiments. YFP was stimulated with an argon laser at 514 nm at 25-50% of its output, and by using neutral density filters at 4-7% to attenuate the laser line. The emission was filtered by using a 530-590 nm band-pass filter. The confocal Z-stacks across time points were aligned by using a multi-modality image registration program, MIRIT, which utilizes information theory to maximize mutual information across image stacks to register at sub-pixel resolution (Maes et al., 1997). The registered stacks were reconstructed in three dimensions, rendered and animated to play continuous movies by using either the Zeiss LSM3.2 or VOLOCITY software (Improvision). The cells in the L1 layer, located at various depths on the curved surface, were projected onto a single reconstructed view by using maximum intensity projection in the VOLOCITY software (Improvision).

Validation of the technique

The older flower buds were removed prior to imaging and the plants were imaged repeatedly at regular intervals. The following criteria were used to assess the performance of plants in our imaging conditions. Dissecting early-stage floral buds can result in desiccation, and such plants were easily recognized and removed from experiments. The vertical growth of the plant was measured at the end of each imaging session by recording the growth in the Z-axis. The plants that stopped growing were not imaged thereafter. The plants that continued to grow but exhibited a gradual and continuous decrease in both the SAM size and the total number of cells were excluded from the analysis. That the conditions used allowed normal meristematic activity was indicated by the following: in all the plants analyzed, no deviation from clonal restriction of cell division patterns in the L1 layer was noticed and the cells continued to divide anticlinally. As in earlier studies, cells in the PZ divide at a faster rate than cells in the CZ. Two studies involving noninvasive sector boundary analysis have shown that the lateral sepals are rarely sectored (Bossinger and Smyth, 1996; Furner and Pumfry, 1993). The sector configurations of flower buds observed in this study correspond well with the configurations obtained in noninvasive methods. The cell expansion behavior observed at the boundary regions mirrors the cell expansion behavior described during the partitioning of leaf primordium from the SAM in *Anagallis arvensis* (Kwiatkowska and Dumais, 2003). The total duration of imaging varied with the imaging intervals, so that when shorter intervals such as 1-1.5 hours and 3 hours were used, the plants were imaged no more than 40-66 hours (n=11 plants). With longer observation intervals such as 6 hours and 12 hours, imaging was performed for 72 (n=5) to 144 hours (n=2).

Results

Fluorescent markers to visualize cell division and expansion

Yellow fluorescent protein (YFP) tags, expressed from promoters active everywhere in the SAM were used to visualize cell division and expansion patterns. Plasma membrane-localized YFP (35S::YFP29-1) represents an EYFP version of 35S::GFP29-1 described earlier (Cutler et al., 2000). The fusion protein is targeted to the plasma membrane and can be used effectively to score for cell division events (Fig. 1A,B). mYFP fused to Histone2B (35S::H2B:mYFP) has been shown to localize to chromatin and hence can be used to monitor nuclear divisions (Fig. 1G,H) (Boisnard-Lorig et al., 2001). A third marker is CyclinB1;1:GFP, which represents a GFP fusion to an *Arabidopsis* mitotic cyclin expressed under its own promoter. The fusion protein is expressed in cells in the G2-M transition, and can be used as a marker for cells about to enter, or in the process of, division (Fig. 3A,B) (Peter Doerner, personal communication). Monitoring the duration of M phase in the cell cycle of SAM cells by using 35S::H2B:mYFP shows that it lasts for less than an hour (Fig. 1G,H). This dictated that the time-lapse intervals used should be 1-1.5 hours, in order to identify all the dividing cells over a period of time. In the case of the plasma membrane marker, the cell division event could be scored as late as 12 hours (Fig. 1A,B) after the event and hence our time-lapse interval was 3 hours, 6 hours or 12 hours in different sets of experiments. The SAM is a dome-shaped multilayered tissue consisting of three clonally distinct layers of cells. We tested whether it was possible to identify cell division events in all three layers. It is possible to identify cell division events in all the cells in the L1 layer (Fig. 1A,B) and in the L2 layer (Fig. 1C,D), and cells located in the corpus (Fig. 1E,F). The floral stages were defined based on morphological criteria; the visible bulge on the meristem flank is considered to be P1 (Fig. 1J K) and the extension of the bulge in the X-Y dimension and appearance of the first sign of a groove between the primordium and the meristem is considered to define P2 (Fig. 1K,L).

Temporal variation in mitotic activity

In the SAM, the CZ is thought to harbor slowly dividing initials and their progeny cells, which can be displaced into the PZ where they differentiate, producing an organ primordium approximately every 24 hours (Smyth et al., 1990). The amounts of cell division were quantified as a function of time from a time-lapse series of individual plants imaged at 6 hours or 12 hours, or 1 hour and 15 minute intervals (Fig. 2A,B,C). All the cells located in the meristematic dome were considered, excluding the ones located in organ primordia from P2 onward.

The mitotic activity within a SAM is not uniform across time. The SAM exhibits periods of relatively rapid cell divisions interspersed with periods of low mitotic activity. Cell division activity in L1, L2 and corpus showed coordinated temporal variations (Fig. 2C). For plants in which imaging was possible for up to 6 days, the low and peak periods of activity could be clearly resolved (Fig. 2A, SAM1; Fig. 2B, SAM5). These plants did not show six peaks of mitotic activity that would approximately correspond to six plastochrons. This suggests that the pulses of mitotic activity are not correlated with the times when each of the primordia arises. Additional observations of transient peaks of cell division rate were made (Fig. 2A, SAM3, SAM4), but these plants were not followed for a long enough period to see multiple activity peaks. It has been reported that cell division activity is subjected to diurnal variations (Lyndon, 1998). We did not detect any striking diurnal variations in time-lapse experiments performed with short intervals (Fig. 2C). Therefore the differential mitotic activity appears to be uncoupled both from the temporal sequence in which each primordium is specified and also from diurnal rhythms, in plants grown under continuous light.

In order to test whether the apparent variations are in part due to the markers used, a cyclinB1;1:GFP construct was used to visualize mitotic cells at various time points. CyclinB1;1:GFP expression dynamics in SAMs were determined by counter-labeling cyclinB1;1:GFP shoot apices with FM4-64, a water-soluble lipophilic dye, to visualize cell divisions. In an individual cell cyclinB1;1::GFP is seen as a

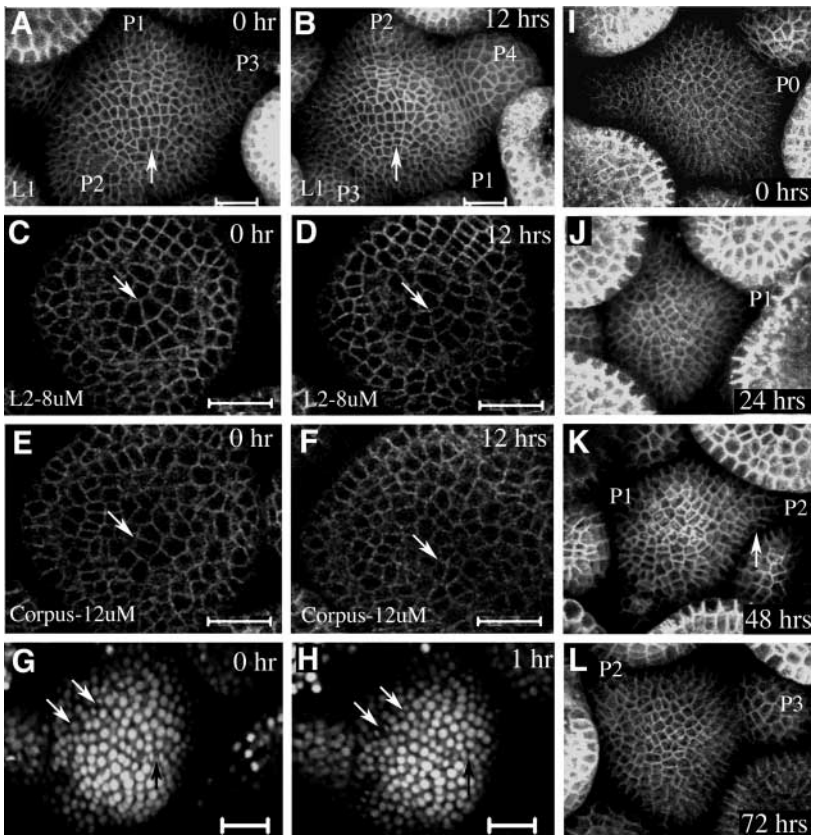

Fig. 1. Cell division markers. (A-F) 35S::YFP29-1 expression in different clonal layers of SAMs. (G-H) 35S:H2B:mYFP expression in reconstructed L1 layer. (A,C,E,G) The first time points (0 hour) and (B,D,F,H) represent the same SAMs after the elapsed time indicated on top right-hand corner of each panel. (A,B) The reconstructed Z-series revealing all the cells in the L1 layer. Primordia at different stages of development are marked as P1, P2, P3. Arrows indicate the same cells prior to and after division. (C,D) Cells in the L2 layer (8 μm deep); the arrow points to cell division events. (E,F) Cells in the corpus (12 μm deep); the arrows point to cell division events. (G,H) The reconstructed images of the L1 layer expressing 35S::H2B:mYFP. Arrows in G indicate cells in division, and arrows in H are the same cells after an hour, showing decondensed chromatin after completion of mitosis. (I-L) Reconstructed views of different growth stages of the same SAM after 24-hour intervals. The earliest visible bulge on the meristem flank is considered as stage P1 (J,K). The extension of the bulge in the *x*/*y* axis and the appearance of a first sign of a groove between the SAM and the primordium is considered stage P2. Scale bar: 20 μm.

bright nuclear label prior to division (Fig. 3A). It then accumulates as a thin line, resembling chromatin at the metaphase plate (Fig. 3B). An hour later cyclin:GFP expression disappears, with concomitant appearance of a new cross-wall (Fig. 3C). Several plants were tested for cyclinB1;1:GFP expression, and a wide range in the number of cyclin-positive cells across different SAMs was observed (Fig. 3D-F). Plants with very few cyclin-expressing cells (Fig. 3D) to intermediate (Fig. 3E) to high levels (Fig. 3F) were observed. A similar variation in mitotic activity across plants has been reported in earlier studies (Laufs et al., 1998; Grandjean et al., 2003). Therefore it can be concluded that the observed temporal variation in mitotic activity is not due to the markers used, but represents real variation.

Spatial distribution of cell division

Primordia arise in a temporal sequence from definite locations within the PZ. Therefore we represented the temporal sequence of cell divisions in space. To do this, time-lapse data were utilized to integrate every cell division event in successive 12-hour windows. These data were projected onto the final time point to generate a spatial map of the mitotic progression in the L1 layer (Fig. 4A-C). The striking feature in such a representation is that cell division is uniformly distributed across the meristem, without any preference for the regions of primordial specification marked P0 (the youngest primordium), P-1 (the position where the primordium after P0 will form) and P-2. A few cells undergo a second round of division within a 36-hour window (Fig. 4C-G, arrows). Time-lapse data (144 hours) from four different plants were analyzed and showed a similar distribution. No spatial preference of cell division activity was observed during both the low (Fig. 4A) and the peak (Fig. 4C) phases. Within this global uniform distribution, however, adjacent cells located in a discrete spatial domain can divide simultaneously or within a short time frame, suggesting a role for local signals in communicating cell division information within a layer (Fig. 4A-C; Movies 1 and 2 at http://dev.biologists.org/supplemental).

Since the SAM is a dome-shaped structure, it is not possible to represent all the cells in the L2 and corpus in a single reconstructed two-dimensional image. Therefore integrated data for 36 hours were projected onto the final time point using optical sections at different depths, as shown (Fig. 4D-G). There is a similar uniform distribution of cell division patterns in the L2 and corpus. However, a representation of mitotic activity over 36 hours was not sufficient to calculate the mitotic index in primordial regions because it was not possible to determine the boundaries of successive incipient primordial regions. Therefore, the lineage analysis was carried out on time-lapse observations spanning over 5 days in order to determine the sectors of the meristem that will ultimately become part of the primordium (Fig. 6A-E, following section). The cumulative mitotic index (CMI) was scored in successive 24-hour intervals, in sectors corresponding to the sites in transition from P-2 to P-1 (Fig. 4H-J), P-1 to P0 (Fig. 4H-J), from P0 to P1, from P1 to P2 (Fig. 4I and J) and from P2 to P3 (Fig. 4J) and also in the intervening regions (IR) (Fig. 4H-J). The CMI is taken as the number of dividing cells over the total number of cells present in individual sectors, over a 24-hour interval. The CMI corresponding to the respective stages was then integrated by averaging the CMI observed in primordia of the same stage; this value was projected onto the final time point (Fig. 4J; Table 1).

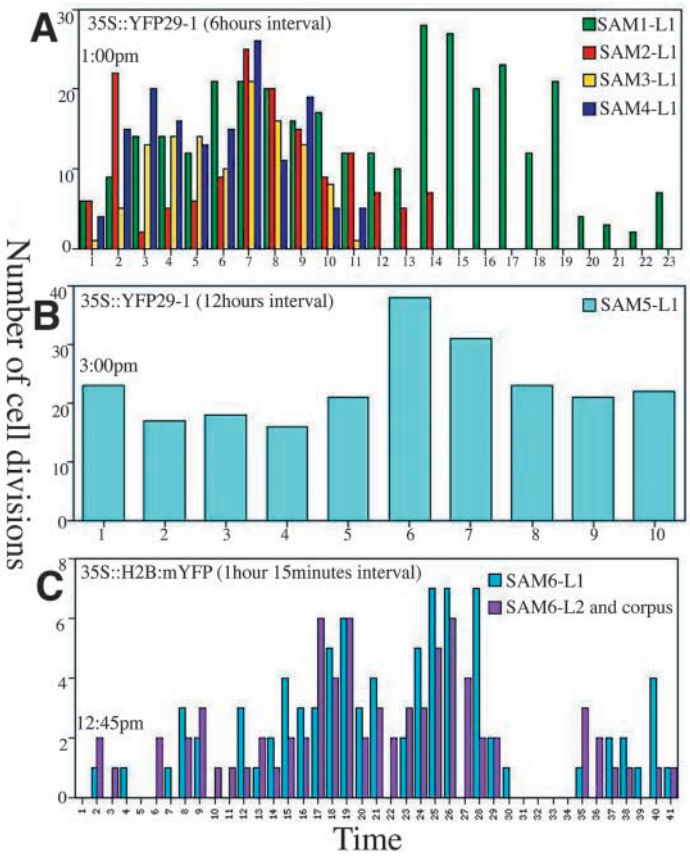

Fig. 2. Temporal variation in mitotic activity in SAMs. (A) Raw data on the number of dividing cells in the L1 layer of four different SAMs (SAM1-SAM4) imaged at 6-hour intervals. In case of SAM2, the data were analyzed only until interval 14 and in case of SAM3 and SAM4 only until interval 11. (B) Data from a plant imaged every 12 hours. (C) Comparison of cell division activity in the L1 layer with that in the L2 layer and corpus of the same plant, imaged every 1 hour and 15 minutes. The number of cell divisions within each time interval is presented. The time at the beginning of the experiment and the cell division marker used are indicated in each case. In each case, note the differences in *y*-axis dimension, which represents number of cell divisions.

Such a dynamic integration of 72 hours of time-lapse data revealed that the mitotic index was comparable among primordia at different stages of development, starting from P-1 to P2. The average CMI for a 24-hour interval among these stages ranged between 67 and 73% (Table 1). However, the CMI in these sectors in any single 24-hour window can range between 45 and 88%, depending on the incidence of active or relatively inactive phases of cell division in the SAMs. The average CMI in regions located between these sectors also showed no significant deviation (Table 1, Table 2). However, the transition from P2 to P3 is marked by a dramatic increase in CMI, which can be as high as 193% for a 24-hour interval (Fig. 4J; Table 1) and such a rapid burst of cell division activity in P3 and later stages can be visualized in continuous movies (Movies 1 and 2 at http://dev.biologists.org/supplemental). Similar bursts of cell division activity were observed in the L2 layer and corpus. In summary, the amount of cell division is comparable in different regions of the SAM until P2 and then a dramatic increase in cell division is observed in P3 and later stages.

Cell cycle length

A combination of mitotic index and cell cycle length is considered to be a good indicator of mitotic activity (Lyndon, 1998). Cell cycle length for every cell was calculated by accounting for the time taken between successive divisions. Ninety-six hours of time-lapse data were taken at 6-hour intervals for this analysis. The frequency distribution revealed a wide range of cell cycle lengths, ranging from between 12 and 18 hours to between 90 and 96 hours (Fig. 5D). However, the majority of the cells have a time between divisions of 12-36 hours.

We projected the data onto the meristem surface to get an idea of the relation between the spatial distribution of cells and their cycle time (Fig. 5A-C). Each of the colors represents a window of cell cycle length. As expected, the cell cycle length was shorter in cells located in the PZ compared with those in the CZ. A majority of the cells in the PZ have a cell cycle length of 18-36 hours. Adjacent cells tend to have similar cell cycle lengths. Within the PZ, marginal differences in cell cycle lengths were observed between early primordial regions (marked as P-1 and P-2 at time 0 hours) and the intervening regions located between two successive primordia. A subset of cells in the primordial regions exhibit a marginally shorter cell cycle length (white arrows in Fig. 5A,B) compared with the intervening region (arrowheads in Fig. 5A,B). This difference is not,

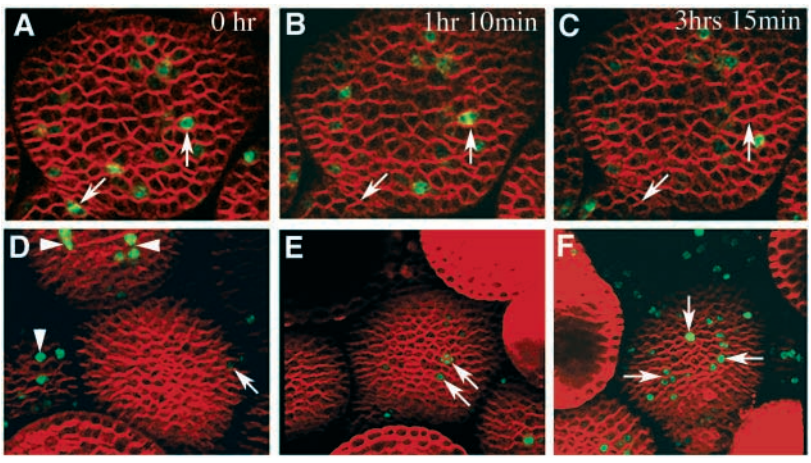

Fig. 3. Differential mitotic cyclin expression in SAMs. (A-C) The same optical section of an L2 layer from a time-lapse series. (A) First time point; (B,C) subsequent time points. The total time elapsed is indicated at the top right-hand corner. In all panels, red represents FM4-64 staining of plasma membranes, and green represents expression of cyclinB1;1:GFP. Arrows in (A-C) point to the same cells over time. (D-F) The reconstructed L1 layer of SAMs from different plants. Arrows point to cyclin-positive cells in SAMs and the arrowheads point to cyclin-positive cells in flower buds.

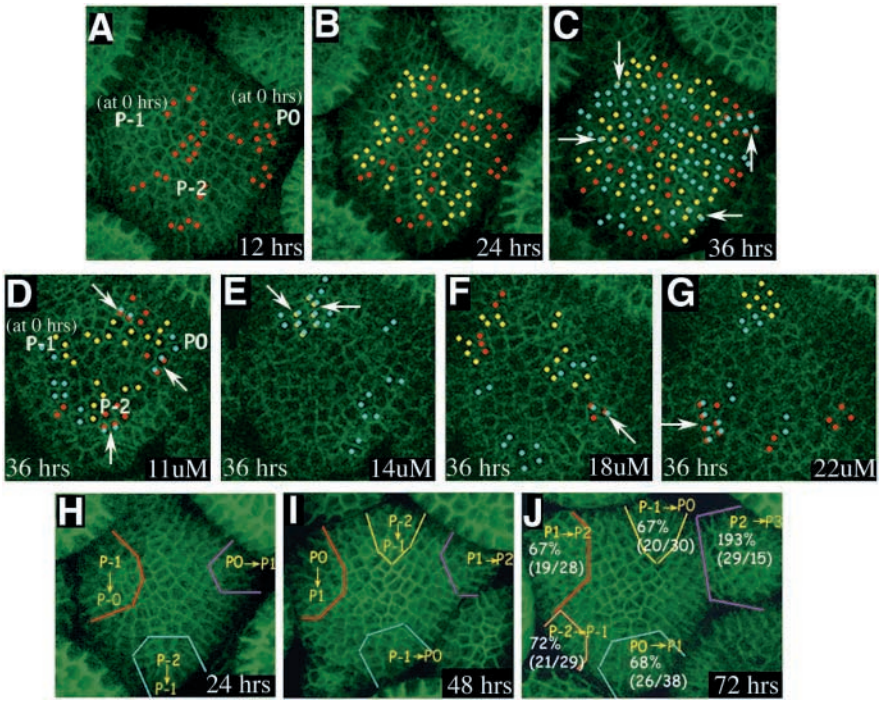

Fig. 4. Spatial distribution of mitotic activity over time. (A-C) A reconstructed L1 layer of the same plant separated by 12-hour intervals. Cells that have divided in each of the intervals are differentially color-coded. Red dots represent cells that divided in the first 12-hour window, yellow dots the following 12 hours, and blue dots the final 12 hours. (D-G) Individual optical sections from the same plant, depicting cells located in the L2 and the corpus from the same time point as in (C), and the color code remains the same. The overlapping dots indicate a second round of cell division (arrows).
(H-J) Reconstructed views of the L1 layer of the same SAM followed over 72 hours. The total elapsed time is marked in individual panels. Different colored sectors represent regions of primordium development marked as stages in transition from P-2 to P-1, from P-1 to P0, from P0 to P1, from P1 to P2 and from P2 to P3. The numbers expressed as percentages in (J) represent averaged cumulative mitotic index calculated for every 24-hour interval over 72 hours, in sectors representing primordia at the same stages. The numbers in parentheses indicate the number of cell divisions over the total number of cells.

however, reflected in the overall primordial CMI. The transition between P2 and P3 is marked by a dramatic decrease in cell cycle length in most of the participating cells (Fig. 5C). Cells that exhibited a cell cycle duration of 24-36 hours until the P2 stage shift to divide every 12-18 hours when in the P3. A similar frequency distribution was observed for cells located in the L2 and corpus. A striking feature associated with this shift in cell cycle length between P2 and P3 is the coordination of cell division among neighboring cells both within and across clonally distinct layers (see Movies 1 and 2 at http://dev.biologists.org/supplemental).

The distribution of cell cycle length in the CZ revealed a pattern in striking contrast to that in the PZ. The range of cell cycle duration in the CZ is much wider than that in the PZ, starting from 36-72 hours. The most slowly dividing cells in the CZ are not arranged in a well-defined concentric circle. Adjacent cells in the CZ can show very different cell cycle lengths. For example, a cell with a previous cell cycle duration of 66-72 hours can share its walls with cells whose previous cycle duration ranges between 36-66 hours. One of the reasons for such a wide range of cell cycle duration could be that the location of the CZ is not constant. Future experiments involving an operational marker for the CZ such as CLV3 might yield insights into the cell division behavior of these cells. In summary, the cell cycle duration in the PZ is relatively uniform compared with that in the CZ. Within the PZ, cell cycle duration is marginally shorter in early primordial regions compared with the cells in the intervening region, with a dramatic decrease in P3 and later stages. This analysis is consistent with the earlier observation that the amount of cell division is similar in regions where successive primordia arise.

Table 1. Average cumulative mitotic index (CMI) for a total duration of 72 hours, in different sectors within the meristem

Sectors within the SAM	Average cumulative motitic index (CMI)
P-2 to P-1 (*n*=3)	72.9% (21.3 s.d.; 15.1 s.e.m.)
P-1 to P0 (*n*=3)	67.3% (19.1 s.d.; 11.0 s.e.m.)
P0 to P1 (*n*=3)	68.2% (14.1 s.d.; 12.5 s.e.m.)
P1 to P2 (*n*=2)	69.5% (13.3 s.d.; 7.6 s.e.m.)
P2 to P3	193%
IR (*n*=5)	67% (17.2 s.d.; 7.69 s.e.m.)

The CMI is taken as number of dividing cells over total number of cells present in individual sectors for a 24 hour interval. The CMI corresponding to the respective stages was then integrated by averaging the CMI observed in individual 24 hour windows and expressed in percentages. Number of respective stages averaged is given in parentheses. The average CMI corresponding to the intervening regions (IR) located between primordial regions is also given. s.d., standard deviation; s.e.m., standard error of mean.

Lineage analysis on time-lapse observations

One of the poorly understood aspects of meristem morphogenesis is the cell behavior associated with the origin

Table 2. Percent increase in cell number during primordial development over time

	P-1 (%)	P-2 (%)	IR (%)
24 hours	171 (12/7)	160 (8/5)	160 (8/5)
48 hours	285 (20/7)	300 (15/5)	240 (12/5)
72 hours	414 (29/7)	400 (20/5)	380 (19/5)

The CMI was calculated only for the progenitor cells in primordial region P-1, P-2 (only five cells that will ultimately constitute a predominant part of the flower bud are considered) and the intervening region (IR) located between them (progenitors for the P-4 region) (Fig. 6A; Fig. 9A,B). The CMI observed in individual sectors during successive 24 hour intervals is expressed as percent increase in cell number over initial number of cells at 0 hours.

and subsequent development of primordia from specialized regions in the PZ. The plant hormone auxin and its distribution have been implicated in the selection of sites of primordium specification (Benkova et al., 2003; Reinhardt et al., 2003b). Lineage analysis has indicated the number of primordium initials (Bossinger and Smyth, 1996). Among the questions that remain are: Where are the primordium initials located? How do they divide? What makes these cells different from the intervening cells located between successive primordia? What is the cell behavior associated with the separation of primordia from the SAM? These questions were addressed by lineage reconstruction from time-lapse observations.

The 35S::YFP29-1 transgene is uniformly expressed throughout the shoot apex, its use as a transgenic fluorescent marker facilitated the tracking of lineages originating from the regions close to the CZ and ending in differentiated primordia (Fig. 6). Time-lapse data from plasma membrane-localized YFP taken at 6-hour intervals over a period of 5 days were used to serially reconstruct lineages in the SAM. Data taken at 3-hour intervals for a period of close to 3 days were used to create continuous four-dimensional movies to reveal essential features of morphogenesis in relation to cell behavior (see Movies 1 and 2 at http://dev.biologists.org/supplemental).

Primordial progenitor cells map close to the slowly dividing cells in the CZ

The time-lapse series allowed the tracking of individual lineages that result in primordial development from very early stages, even before any visible appearance of primordial outgrowth. The time series of an entire three-dimensional Z-stack was registered sequentially onto subsequent time points by using a multimodality image registration algorithm in order to achieve cell-by-cell alignment at sub-pixel resolution. This allowed superimposition of the corresponding cells in the SAM across time points. Such aligned stacks were used to trace lineages in the meristem that lead to floral primordia. The L1 lineages incorporated into the successive primordia within one SAM are depicted in Fig. 6. Each one of the color-coded dots represents a progenitor cell in the 0 hour image (Fig. 6A), and the lineages that result from the divisions of these cells and their descendents are marked with the same color code (Fig. 6B-E). We compared the location of the 0-hour progenitor cells to that of the slowly dividing cells in the CZ. In most cases they abut these cells. The number of cells that give rise to P-1 and P-2 was higher and with a progressive decrease with P-3 and P-4 (Fig. 6A), as expected from the continued division of cells from P-4 to P-1. The progenitor cells are arranged in either two rows in a radial arc (P-1 and P-2) or at earlier stages as a single row (P-4). Although we were unable to determine the differentiation status of the primordium progenitor cells, the mapping of progenitor cells close to the CZ allowed us to follow the entire sequence of PZ cell behavior from early divisions to primordium development.

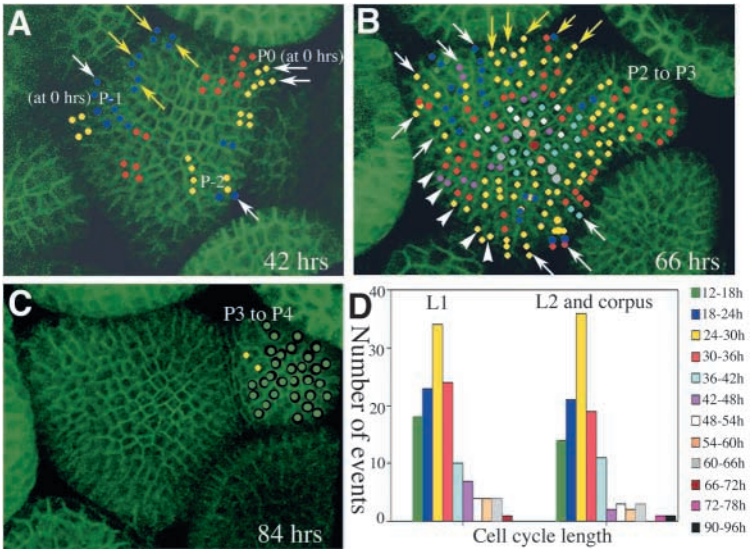

Fig. 5. Frequency and spatial distribution of cell cycle length. (A-C) Reconstructed views of the L1 layer of the same plant, expressing 35S::YFP29-1, over a period of time. (D) Frequency distribution of cell cycle length among cells in the L1 and in the L2 and corpus together. Each of the color-coded bars represents a window of cell cycle length and each one of them is separated by 6 hours. Such individual events are mapped onto the L1 layer of the SAM in A-C, by marking both of the siblings. In cases where a single dot can be seen, the cells divided in the subsequent time interval. The color code employed in the spatial representations is the same as that used in representing the frequency distribution. The stages in A represent the ones at the beginning of the experiment. The stages marked in B and C are the ones in transition from P2 to P3 and P3 to P4, respectively. Elapsed time is indicated on each panel. White arrows point to cells in primordial regions P0, P-1 and P-2. White arrowheads point to cells in the intervening region located between P-1 and P-2. Yellow arrows point to cells in the intervening region, located between P0 and P-1. The cells marked in regions P-1 and P-2 (A, white arrows) are also represented in the next panel (B, white arrows) to maintain continuity.

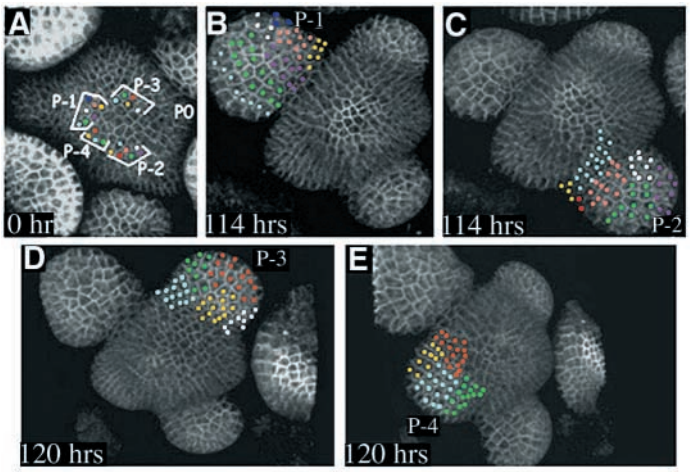

Fig. 6. Location of primordium progenitor cells. (A-E) Reconstructed view of the L1 layer of a shoot apex expressing 35S::YFP29-1, with (A) being the first time point and elapsed time in (B-E) marked on individual panels. (A) Initials that give rise to individual primordia (P-1, P-2, P-3 and P-4) are shown in enclosed areas marked in white. The progenitors of a given primordium are color-coded. (B-E) Primordia that have developed from the progenitors marked in A. Individual lineages within a primordium are color-coded. The same color has been used for each progenitor and its descendants.

Oriented cell divisions associated with axis of primordial outgrowth

A full-time series of projected sections depicting successive cell divisions in L1 cells that gave rise to two primordia is represented (Fig. 7A-F). Successive divisions in the earliest cells and their descendents were oriented away from the CZ and divided parallel to the lateral axis of primordial outgrowth as shown for P-1 (Fig. 7D). The first set of oriented cell divisions was observed between 12-18 hours within the P-1 sector. Such oriented cell divisions in the following 24-30 hours resulted in a column-shaped lineage and in extension growth of the primordium from P-1 to P1. A similar pattern was visualized for the subsequent primordia: for example, P-2 in the same shoot apex (Fig. 7G-L). While most of the progenitors consistently divide parallel to the axis of primordial outgrowth, the first divisions in the most laterally located cells (white and pink in the figure) are random with later divisions oriented parallel to the axis of primordial outgrowth (Fig. 7G-L). Similar observations were made for the P-3 region (data not shown). The division orientation of the cells in the PZ located between primordial progenitors was also measured; in this case the region is marked as P-4 and it is located between P-1 and P-2 (Fig. 6A). The cell division analysis in these cells revealed a contrasting pattern in comparison with the cells that form the next set of primordia. The cell division patterns of P-4 cells that occurred over a period of 66 hours are projected onto the final time point in Fig. 9A,B. Cells in the intervening regions divided in random orientation and the resultant lineages appeared as square blocks rather than as columns of cells. For simplicity in comparison, the lineages in the rest of the meristem are not represented, although similar differential patterns of cell division did occur there. However, not all of the lineages that follow oriented cell divisions ultimately became part of primordia (for example, the lineage marked in blue in Fig. 7L, which was retained in the SAM proximal to the primordium, and only a part of the lineage marked in yellow became part of the primordium). This observation suggests that the axis of growth does not entirely constrain the fate of these lineages. Seven plastochrons from two different plants were examined and all of them revealed similar cellular behavior. Similar analysis was carried out on cells in the L2 layer, and the resultant lineages were projected onto the final time point. Since it was not possible to represent all the cells located at different depths in the L2 layer in one section, the cells were represented in individual optical sections at different depths (Fig. 8B-D). This analysis revealed that cells preferentially divided parallel to the axis of primordium growth. Even though individual cell divisions in the corpus could be followed, it was not possible to serially reconstruct complete lineages due to a lack of resolution in the distal-most regions, owing to the curvature of the SAM. However, cells located in the corpus region of primordia in P3 stages could be mapped; this corresponds to the time the flower primordium begins to acquire height. During these stages, periclinal divisions could be observed

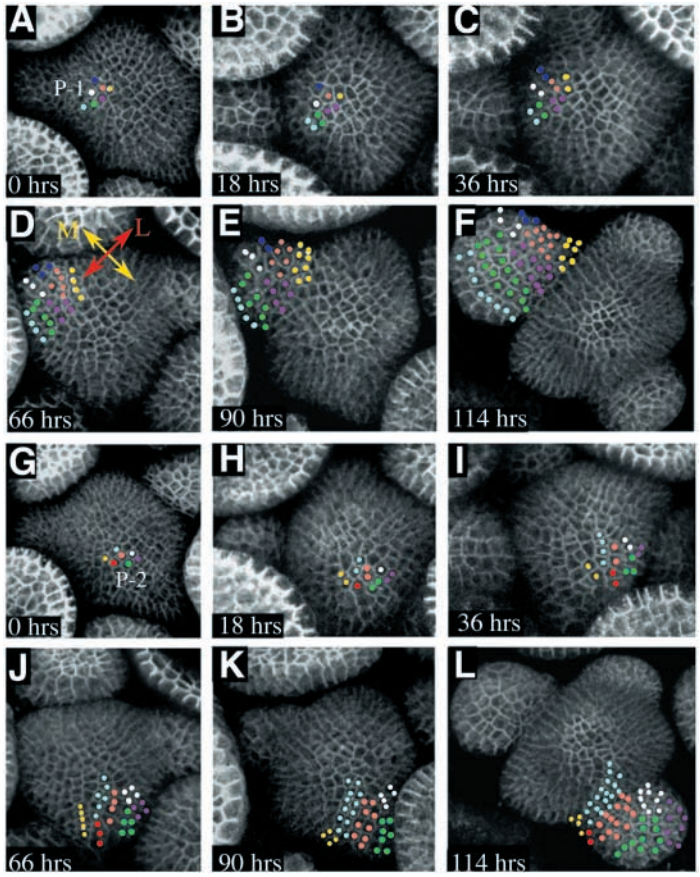

Fig. 7. Cell division patterns in primordium progenitors and their descendents. (A-F) Reconstructed views of the L1 layer of the same SAM expressing 35S::YFP29-1, over a period of time. The elapsed time is indicated in individual panels. Cells of individual developing lineages are marked in different colors. (G-L) represents a similar analysis of the P-2 region of the same shoot apex. The lateral (L in red) and the medial (M in yellow) axis of the developing flower primordium are marked in (D). The cell division axis in primordial progenitors is referenced as parallel to the lateral axis of the flower primordium.

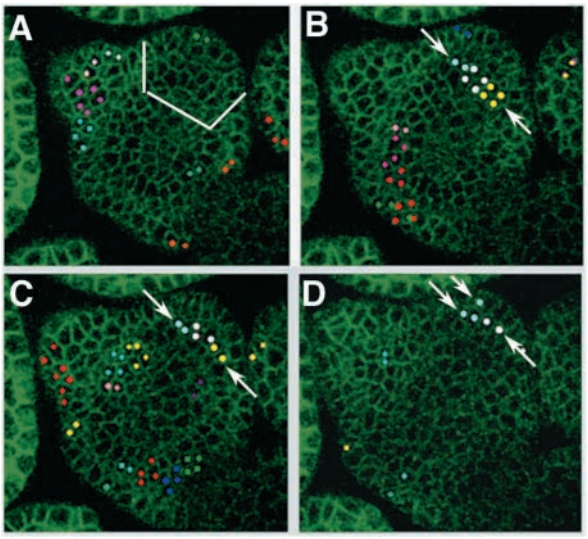

Fig. 8. Cell division patterns in the L2 layer. The cell division patterns that occurred in the L2 layer of a primordial region is presented. Such cell division patterns are projected onto the final time point. (A-D) Sections at different depths in the SAM. The structure of the lineages leading to each primordium (white boxed region) is represented. Three different lineages are color-coded and the arrows point to sibling cells located at different depths.

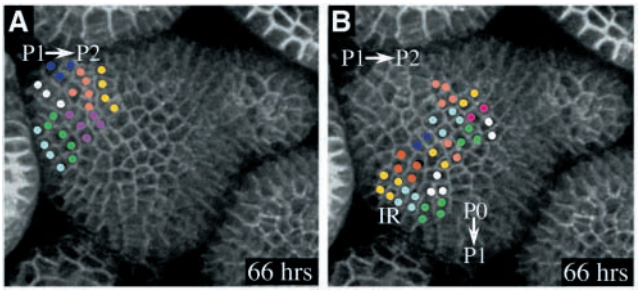

Fig. 9. Cell division patterns in cells located between developing primordia. (A,B) Reconstructed view of the shoot apex of the same plant at the same point in a time series. Elapsed time from the initial observation is marked. The lineages that result in a primordium in transition from P1 to P2 are marked in (A), while the lineages in the intervening region (IR) between two successive primordial regions P1→P2 and P0→P1 are marked in (B). Individual lineages are differentially color-coded.

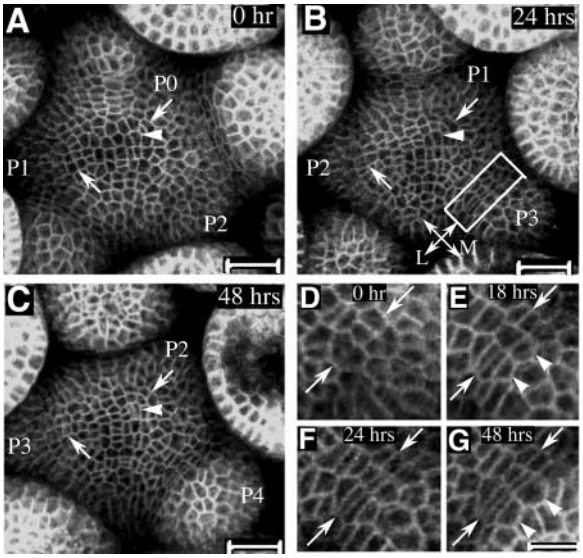

Fig. 10. Cell expansion patterns and cell behavior at the boundary region. (A-C) Reconstructed views of a SAM expressing 35S::YFP29-1, from a time series. Total elapsed time is indicated in individual panels. Arrows point to the same cells in the PZ over a period of time, and they divide along their long axis. Arrowhead points to a cell in the CZ dividing along its short axis. The white-boxed area in (B) represents the boundary region. Magnified view of a time-lapse series of the boundary region is shown in (D-G). The total elapsed time is marked on individual panels. Arrows indicate the same cells in the boundary region across time. Arrowheads indicate adjacent cells in the developing flower primordium. The lateral (L) and the medial (M) axis of the developing flower primordium are marked in B. Scale bar: 20 μm in A-C; 10 μm in D-G.

in the corpus. In summary, this analysis links cell division orientation changes to the initial stages of primordium outgrowth.

Dynamic re-orientation of cell division axis in intervening cells

Cells in intervening regions (P-4) (Fig. 6A), which divided in random orientation at the time (1-66 hours) when their neighbors exhibited oriented cell divisions (Fig. 9B), were followed to observe the change from random to oriented division. P-4 progenitor cells changed their planes of division and oriented parallel to the axis of primordium outgrowth between 72 and 120 hours (compare yellow, blue and green lineages in Fig. 9B with Fig. 6E). This reveals that cells adjusted their cell division planes in response to temporal signals related to primordia development.

Cell expansion patterns

Cell expansion is another critical aspect of growth, and it has been proposed to play a key role in SAM morphogenesis. Cell expansion patterns in different stages of primordium development were examined. The cells in the primordial regions expanded along the medial axis of primordial outgrowth and divided perpendicular to the axis of cell expansion (Fig. 7A-D). We have not yet developed software to quantitate cell size. However, rapid cell expansion could be observed during P2 and later stages, in continuous movies, as the distance between adjacent nuclei increased rapidly (see Movie 1 at http://dev.biologists.org/supplemental). At the P3 stage the cells located in the primordium continued to expand rapidly compared with cells located in the groove between the primordium and the SAM, which is referred to as the boundary region (Fig. 10B, boxed area, and C; see Movies 1 and 2 at http://dev.biologists.org/supplemental). This behavior can be readily seen in higher magnification images (Fig. 10D-G). The cells located in the boundary region failed to expand along the medial axis of the flower bud following division, while they appeared to expand along the lateral axis (arrows in Fig. 10D-G). The differential cell expansion resulted in a column of cells that appeared elongated along the lateral axis and contracted along the medial axis of the flower bud. Meanwhile, the cells that lined the medial edge of the primordium expanded rapidly in both directions (arrowheads in Fig. 10E-G point to the same cells over a period of time). This rapid cell expansion was followed by a burst of coordinated cell division in the cells of the primordium (Movie 2 at http://dev.biologists.org/supplemental; the red open arrow points to the boundary region, while the closed red arrow points to cells in the primordium). It was during this time that the flower primordium 2 (P2), which was only an extension of the meristem in the X-Y dimension, began to acquire height, eventually leveling off at the height of the SAM. The sustained growth of the flower primordium P3, thereafter bordered by a non-growing boundary region, ultimately resulted in complete separation of the primordium from the meristem, with the boundary region forming a continuous layer with the pedicel (see Movie 2 at http://dev.biologists.org/supplemental, P3). Similar cell behavior could be seen in cells that formed the boundary regions in layers below the L1 (data not shown).

In summary, distinct cell behavior is associated with different stages of primordium development. Oriented cell divisions, in primordial progenitors and in cells located proximal to them is associated with initial primordial outgrowth, and this is followed in turn by a rapid cell expansion in cells of primordia of the P2 stage. The continued rapid cell expansion in P3 and in later stages, coupled with a rapid burst of cell division, transforms the P2 primordium into a later-stage flower bud. At the same time, cells located in the boundary region show no similar growth.

Discussion

Temporal variations in cell division activity

Variation in mitotic index has been observed in several species and is linked to diurnal rhythms (Lyndon, 1998). Our analysis has shown that the cell division activity in SAM is subject to temporal variation. The observed variation in mitotic activity followed neither the temporal sequence in which primordia arose, nor any apparent diurnal rhythms. The variation in windows of differential mitotic activity both within and across plants suggests that they may not be regular. So we do not wish to refer to them as mitotic waves but consider them transient fluctuations in mitotic activity. Such transient temporal variations could arise if they are linked to a signaling mechanism with individual components bound to temporal variations. One such mechanism that operates in the SAM is the meristem maintenance feedback loop involving the CLV and WUS genes. WUS, which has been shown to be a critical regulator of SAM maintenance, is negatively regulated by a hypothetical CLV signaling cascade. WUS in turn positively feeds back onto the CZ region to maintain CLV3 activity (Brand et al., 2000; Schoof et al., 2000). The nature of the regulation involving feedback loops and a dynamic environment might result in transient fluctuations in WUS expression levels and/or domain of expression, which in turn may have an effect on CLV3 expression. It is possible that WUS activity, either directly or indirectly, might influence the mitotic activity in the SAM at any given time. It has been shown that the ectopic expression of WUS results in a fasciated meristem, and expansion of the CLV3 expression domain (Schoof et al., 2000; Brand et al., 2002). However, it is unclear whether expansion of CLV3 expression is a cause or an effect of meristem fasciation. Examining the effects of transient perturbations in feedback loops on both cell division patterns and gene expression domains in real time should yield new insights.

Cell behavior and primordium development

We have given a dynamic description of several aspects of growth: the amount of cell division, cell division orientation and cell expansion patterns associated with SAM morphogenesis. Analysis reveals that it requires a minimum of 4 days of continuous observation to reveal the essential aspects of cell behavior associated with primordium growth. We have mapped the location of primordium progenitor cells to a point early enough that they are close to the slowly dividing cells in the CZ. Sector boundary analysis in inflorescence meristems (IM) of *Arabidopsis thaliana* has led to the prediction that a flower bud arises from a set of four progenitor cells (Bossinger and Smyth, 1996). Our observations show that number of primordium progenitor cells varies across successive plastochrons, as must be true if the cells continue to divide. The progenitor cells that represent the primordium at stages P-1 and P-2 are higher in number than those comprising primordia at stages P-3 and P-4. Therefore, number of primordium progenitors in our time-lapse experiments is determined by the stage at which the progenitor cells are observed. Ultimately, a lineage originating from a single cell might result in a primordium, as proposed by Bossinger and Smyth (Bossinger and Smyth, 1996). The limited duration of our time-lapse observations prevented us from observing such a cell. Furthermore, our results do not reveal when primordial progenitor cells become determined to a primordial fate. However, we can ask the question: what is the stage at which the progenitor cells begin to divide predominantly in an oriented manner, and become exclusively primordial in fate? The answer is no later than a stage between P-1 and P0 (Fig. 6A,B), when the progenitor cells exhibit oriented cell divisions, and all the lineages originating from them become part of a flower bud (Fig. 7A-F). Oriented cell divisions are not necessarily a useful criterion for the first signs of primordial differentiation or determination, however, because not all the lineages that exhibit such a division pattern ultimately become part of the primordium. Answers to questions of time of the earliest differentiation of primordial cells will require a combination of a range of carefully defined cell-type-specific markers with cell division analysis. Such an effort has been made in a recent study by observing *LEAFY(LFY)*-expressing cells through a live-imaging approach (Grandjean et al., 2003). It was shown that the *LFY* expression domain is established gradually through cell recruitment, and *LFY* was found to be expressed in a broader domain than the primordial progenitors. Therefore, it was not possible to determine the number or exact location of primordial initials. Recent studies have demonstrated that auxin distribution in the SAM, mediated by auxin efflux carrier *PINFORMED1 (PIN-1)* predicts the sites of primordium initiation (Benkova et al., 2003; Reinhardt et al., 2003b). It has also been shown that *PIN-1* expression is established at least a plastochron earlier than *LFY* expression (Reinhardt et al., 2003b). Therefore, early auxin response genes might act as more useful markers.

Since we were able to identify the progenitor cells early in primordial development by tracing back to early stages, we could follow the cell behavior associated with primordium development in relation to the rest of the cells in the SAM. Our analysis of both the temporal and spatial patterns of cell division activity, and of cell cycle length revealed that the amount of cell division is comparable in regions of primordial development. This observation is in contrast with that described earlier for *Arabidopsis* SAMs (Laufs et al., 1998). The analysis in that paper indicated that cell division is not uniformly distributed in a SAM, and that twice the amount of cell division occurs in the predicted P0 sector compared with the P-1. The apparent contradiction could be due to the differences in technique, as the earlier analysis was not dynamic and the temporal variations in mitotic rate within a given SAM might introduce errors upon averaging single time point observations taken from different plants. Other possibilities, such as differences in staging of the primordia and our averaging cell divisions over 24-hour intervals, which may not precisely correlate to each plastochron, might contribute to the different observations made in this study. However, such possibilities should not have influenced the conclusions drawn in this study because the primordial regions were followed simultaneously, in continuous observations. The striking similarities in the rates of cell division at each one of the time windows, irrespective of averaging, can be seen by following individual cell divisions in primordial regions P-1 and P-2 starting from 0 hours to 66 hours (compare Fig. 7A-D with 7G-J), and such a similarity is also reflected in similar cell cycle lengths (Fig. 5A,B, white arrows). The definition of primordial boundaries is based on lineage restriction to the flower bud. It

was possible to determine the primordial boundaries at a single cell resolution in cases such as P-1 (Fig. 6B), but it was not the case in the P-2 region, as only a subset of the lineages marked in yellow and blue became part of the flower bud (Fig. 6C). Therefore, although the determination of future primordial boundaries cannot be done at single-cell resolution earlier than stage P-1, this may not affect the conclusions drawn in this study. An additional question is: what is the rate at which the PZ cells divide in the intervening region, located between successive primordial regions? The differences in cell cycle lengths in the intervening region located between the P0 and P-1 sectors were not strikingly different when compared to either one of the primordial regions (Fig. 5A,B, compare regions of P0 and P-1, marked in white arrows, with the intervening region marked in yellow arrows). However, a subset of cells in primordial regions P-1 and P-2 (Fig. 5A,B, white arrows) exhibited a marginally shorter cell cycle length compared with the cells in the intervening region located between them (Fig. 5B, arrowheads). The cell division rates in all the primordial progenitor cells and their descendents are not uniform. For example, during early primordial growth, a cell with a previous cell cycle length of 18-24 hours may shift to divide every 30-36 hours or even 42-48 hours. A subset of primordium progenitor cells divide relatively infrequently compared with the rest of the progenitor cells, resulting in lineages of different sizes (Fig. 7D,E, compare the lineages marked in white and blue with the rest). Similar differences in cell division rates among primordial progenitors and their descendents can be inferred by comparing the sizes of individual lineages in the flower buds (Fig. 6B-E). Such a heterogeneity in cell cycle duration within a floral primordium has been described (Grandjean et al., 2003). Asynchronous cell division among primordial progenitors has been predicted, as an explanation of sector configurations observed in clonal analysis (Bossinger and Smyth, 1996). The comparison of sizes of individual lineages in P2 with that of the intervening region (IR) (Fig. 9A,B) revealed that the lineages in P2 are only marginally larger than those in the IR, which corresponds with the slow formation of the primordial bulge on the meristematic flank (see Movie 1 at http://dev.biologists.org/supplemental; watch for the growth in the P-1 region). However, it can also be argued that the transient local increase in cell division rates in primordial regions could result in the primordial bulge, which in itself is an inconspicuous growth. Our data on cell division rates support such an argument, although such transient differences could not be resolved in the mitotic index analysis.

There is a striking pattern of oriented cell divisions parallel to the axis of primordial outgrowth. Such a pattern of cell division is accompanied by an initial extension of the primordium. Not all the cells that showed such a behavior were ultimately incorporated into a primordium. This suggests that not only the growth axis of primordial progenitor cells, but also the growth axis in cells located proximal to the progenitor cells, might facilitate outward growth. In this context, our results are not in complete agreement with Bossinger and Smyth (Bossinger and Smyth, 1996), with respect to the proposed spatial arrangement of progenitor cells on the meristem flank, and cell division patterns. They propose that the four progenitor cells are arranged as a block and the four cells then divide to generate a concentric group of cells. Such cell division patterns would not explain the outward growth noticed in initial stages of primordium development. Several studies have indicated that structured cell division patterns play a critical role in differentiation and morphogenesis. Recent growth models of *Antirrhinum* petal lobes reveal that the generation of asymmetric shape depends on the direction of growth rather than on regional differences in growth rates (Rolland-Lagan et al., 2003). It has been shown that the induction of non-anticlinal divisions in the tunica layers of tobacco shoot apices leads to alterations in key regulators of SAM maintenance but fails to induce morphogenesis (Wyrzykowska and Fleming, 2003). However, it can be argued that the maintenance of structured anticlinal divisions in the tunica layer, such as the ones described in this study, might be essential for morphogenesis to occur. Surgical ablation of the L1 layer has been shown to affect cell division patterns in layers below and also to affect primordium development (Reinhardt et al., 2003a). Our results, indicating regular patterns of cell division from early primordial growth, support the idea that planes as well as numbers of cell divisions, are under tight control in the SAM.

We have observed cells dividing perpendicular to the expanding axis in regions of primordial development (Fig. 7A-D). It was not possible, however, to quantify cell expansion patterns. Therefore, we cannot say whether the initial set of oriented cell divisions are a cause or an effect of growth in the primordial regions. The role of cell expansion in SAM morphogenesis has been explored (Pien et al., 2001; Reinhardt et al., 1998). Expansin proteins are upregulated at the sites of incipient primordium formation in tomato meristems, and the local expression of expansins has been shown to induce leaf development in tobacco meristems (Pien et al., 2001). Based on these observations, it has been argued that cell-division-independent mechanisms play a role in morphogenesis. The oriented cell divisions associated with primordium outgrowth in our study could be due to regulated regional expansion resulting in oriented cell divisions. Although regulated cell expansion might initiate such patterning, the gradients of local cell division patterns have to be maintained to sustain further growth. It should be possible to seek a causal link between regulated patterns of cell expansion and orientation of cell division by studying them in real time, with the methods introduced here, after development of image processing methods for measurement of cell size. The studies on the surface expansion of the SAMs, in *Arabidopsis thaliana* and in other species, have yielded quantitative description of cell expansion behavior (Dumais and Kwiatkowska, 2002; Kwiatkowska and Dumais, 2003; Kwiatkowska, 2004). Studies of the vegetative shoot apex of *Anagallis arvensis* and the inflorescence apex of *Arabidopsis thaliana* have shown that the surface expansion in the CZ is slow and nearly isotropic in comparison with that of the PZ, which is found to be greater and anisotropic (Kwiatkowska and Dumais, 2003).

The surface geometry and expansion patterns during early stages of leaf primordium development have been described. Our analysis of cell expansion patterns is not yet quantitative. However, some qualitative observations can be made. We have noticed that cells in the CZ exhibit a relatively proportional expansion in all directions compared with the cells in the PZ (see Movie 2 at http://dev.biologists.org/supplemental). It has been shown that cell expansion is slow in regions that give rise

to the leaf axil, with cells expanding along the axil while contracting across it (Kwiatkowska and Dumais, 2003). It has been proposed that such cell behavior on the adaxial leaf margins of developing primordium would partition the leaf primordium from the surface of the SAM. We have described a similar cell behavior in the boundary regions between flower primordium and the SAM, with cells failing to expand along the medial axis of the flower bud. Therefore, such cell expansion behavior at boundary regions could be a common theme utilized in developmental contexts that require partitioning of actively growing regions, where mechanisms such as programmed cell death (PCD) are not utilized.

Toward a 'digital shoot apex'

One of the major limitations in understanding growth in both plants and animals has been the inability to monitor cell behavior in real time. Several studies have tried to address this issue, starting from inference of cell behavior from clonal analysis, to generative modeling of growth through computer simulations (Resino et al., 2002; Rolland-Lagan et al., 2003). Our analysis of growth in real time circumvents the requirements for inference in studies of clonal growth, or for theoretical growth simulations. Once cell positions can be extracted by cell-finding algorithms, it should be possible to integrate cell coordinates in time-lapse observations. Such efforts are currently in progress (www.computableplant.org). The challenge for the future is to superimpose models of gene regulatory networks on such models of growth, and to integrate with these models the cell–cell interactions involved in meristem maintenance and morphogenesis (Shapiro et al., 2003).

We thank Peter Doerner for sharing the cyclinB1;1:GFP line prior to publication and Jim Haseloff and Sarah Hodge for the 35S::H2B:mYFP construct and Joel Griffitts for making the 35S::YFP29-1. We thank members of Meyerowitz lab for useful discussions and comments on the manuscript. We thank members of Biological Imaging Center (BIC), Caltech: especially Scott Fraser, Andrew Ewald and Hayong Lim for advice and interest in this study. We are grateful to Henrik Jönsson for his help in automating the image registration process. GVR is a fellow of the Jane Coffin Childs memorial fund for medical research. This work was supported by National Science Foundation grants IBN-0211670 and EF-0330786.

References

Ball, E. (1960). Cell division patterns in living shoot apices. *Phytomorphology* **10**, 377-396.

Benkova, E., Michniewicz, M., Sauer, M., Teichmann, T., Seifertova, D., Jurgens, G. and Friml, J. (2003). Local, efflux-dependent auxin gradients as a common module for plant organ formation. *Cell* **115**, 591-602.

Boisnard-Lorig, C., Colon-Carmona, A., Bauch, M., Hodge, S., Doerner, P., Bancharel, E., Dumas, C., Haseloff, J. and Berger, F. (2001). Dynamic analyses of the expression of the HISTONE::YFP fusion protein in arabidopsis show that syncytial endosperm is divided in mitotic domains. *Plant Cell* **13**, 495-509.

Bossinger, G. and Smyth, D. R. (1996). Initiation patterns of flower and floral organ development in Arabidopsis thaliana. *Development* **122**, 1093-1102.

Brand, U., Fletcher, J. C., Hobe, M., Meyerowitz, E. M. and Simon, R. (2000). Dependence of stem cell fate in Arabidopsis on a feedback loop regulated by CLV3 activity. *Science* **289**, 617-619.

Brand, U., Grunewald, M., Hobe, M. and Simon, R. (2002). Regulation of CLV3 expression by two homeobox genes in Arabidopsis. *Plant Physiol.* **29**, 565-575.

Byrne, M. E., Barley, R., Curtis, M., Arroyo, J. M., Dunham, M., Hudson, A. and Martienssen, R. A. (2000). Asymmetric leaves1 mediates leaf patterning and stem cell function in Arabidopsis. *Nature* **408**, 967-971.

Callos, J. D., DiRado, M., Xu, B., Behringer, F. J., Link, B. M. and Medford, J. I. (1994). The forever young gene encodes an oxidoreductase required for proper development of the Arabidopsis vegetative shoot apex. *Plant J.* **6**, 835-847.

Clark, S. E., Running, M. P. and Meyerowitz, E. M. (1993). CLAVATA1, a regulator of meristem and flower development in Arabidopsis. *Development* **119**, 397-418.

Clark, S. E., Running, M. P. and Meyerowitz, E. M. (1995). CLAVATA3 is a specific regulator of shoot and floral meristem development affecting the same processes as CLAVATA1. *Development* **121**, 2057-2067.

Clark, S. E., Williams, R. W. and Meyerowitz, E. M. (1997). The CLAVATA1 gene encodes a putative receptor kinase that controls shoot and floral meristem size in Arabidopsis. *Cell* **89**, 575-585.

Clough, S. J. and Bent, A. F. (1998). Floral dip: a simplified method for Agrobacterium-mediated transformation of Arabidopsis thaliana. *Plant J.* **16**, 735-743.

Colon-Carmona, A., You, R., Haimovitch-Gal, T. and Doerner, P. (1999). Technical advance: spatio-temporal analysis of mitotic activity with a labile cyclin-GUS fusion protein. *Plant J.* **20**, 503-508.

Cutler, S. R., Ehrhardt, D. W., Griffitts, J. S. and Somerville, C. R. (2000). Random GFP::cDNA fusions enable visualization of subcellular structures in cells of Arabidopsis at a high frequency. *Proc. Natl. Acad. Sci. USA.* **97**, 3718-3723.

Dolan, L. and Poethig, R. S. (1998). Clonal analysis of leaf development in cotton. *Am. J. Bot.* **85**, 315-321.

Dumais, J. and Kwiatkowska, D. (2003). Analysis of surface growth in shoot apices. *Plant J.* **31**, 229-241.

Fletcher, J. C., Brand, U., Running, M. P., Simon, R. and Meyerowitz, E. M. (1999). Signaling of cell fate decisions by CLAVATA3 in Arabidopsis shoot meristems. *Science* **283**, 1911-1914.

Furner, I. J. and Pumfrey, J. E. (1993). Cell fate in the inflorescence meristem and floral buttress of Arabidopsis thaliana. *Plant J.* **4**, 917-931.

Gonzalez-Gaitan, M., Capdevila, M. P. and Garcia-Bellido, A. (1994). Cell proliferation patterns in the wind imaginal disc of Drosophila. *Mech. Dev.* **46**, 183-200.

Grandjean, O., Vernoux, T., Laufs, P., Belcram, K., Mizukami, Y. and Traas, J. (2003). In vivo analysis of cell division, cell growth, and differentiation at the shoot apical meristem in Arabidopsis. *Plant Cell* **16**, 74-87.

Hernandez, L. F., Havelange, A., Bernier, G. and Green, P. B. (1991). Growth behavior of single epidermal cells during flower formation: sequential scanning electron micrographs provide kinematic patterns for *Anagallis*. *Planta* **185**, 139-147.

Irish, V. F. and Sussex, I. M. (1992). A fate map of the Arabidopsis embryonic shoot apical meristem. *Development* **115**, 745-753.

Kayes, J. M. and Clark, S. E. (1998). CLAVATA2, a regulator of meristem and organ development in Arabidopsis. *Development* **125**, 3843-3851.

Kwiatkowska, D. (2004). Surface growth at the reproductive shoot apex of Arabidopsis thaliana pin-formed 1 and wild type. *J. Exp. Bot.* **55**, 1021-1032.

Kwiatkowska, D. and Dumais, J. (2003). Growth and morphogenesis at the vegetative shoot apex of Anagallis arvensis L. *J. Exp. Bot.* **54**, 1585-1595.

Laufs, P., Grandjean, O., Jonak, C., Kieu, K. and Traas, J. (1998). Cellular parameters of the shoot apical meristem in Arabidopsis. *Plant Cell* **10**, 1375-1390.

Laux, T., Mayer, K. F., Berger, J. and Jurgens, G. (1996). The WUSCHEL gene is required for shoot and floral meristem integrity in Arabidopsis. *Development.* **122**, 87-96.

Long, J. A., Moan, E. I., Medford, J. I. and Barton, M. K. (1996). A member of the KNOTTED class of homeodomain proteins encoded by the STM gene of Arabidopsis. *Nature* **379**, 66-69.

Lyndon, R. F. (1998). The shoot apical meristem: its growth and development. *Developmental and Cell Biology Series* New York: Cambridge University Press.

Maes, F., Collignon, A., Vandermeulen, D., Marchal, G. and Suetens, P. (1997). Multimodality image registration by maximization of mutual information. *IEEE Trans. Med. Imaging* **16**, 187-198.

Mayer, K. F., Schoof, H., Haecker, A., Lenhard, M., Jurgens, G. and Laux, T. (1998). Role of WUSCHEL in regulating stem cell fate in the Arabidopsis shoot meristem. *Cell* **95**, 805-815.

Meyerowitz, E. M. (1997). Genetic control of cell division patterns in developing plants. *Cell* **88**, 299-308.

Pien, S., Wyrzykowska, J., McQueen-Mason, S., Smart, C. and Fleming, A. (2001). Local expression of expansin induces the entire process of leaf

development and modifies leaf shape. *Proc. Natl. Acad. Sci. USA.* **98**, 11812-11817.

Reinhardt, D., Wittwer, F., Mandel, T. and Kuhlemeier, C. (1998). Localized upregulation of a new expansin gene predicts the site of leaf formation in the tomato meristem. *Plant Cell* **10**, 1427-1437.

Reinhardt, D., Frenz, M., Mandel, T. and Kuhlemeier, C. (2003a). Microsurgical and laser ablation analysis of interactions between the zones and layers of the tomato shoot apical meristem. *Development* **130**, 4073-4083.

Reinhardt, D., Pesce, E. R., Stieger, P., Mandel, T., Baltensperger, K., Bennett, M., Traas, J., Friml, J. and Kuhlemeier, C. (2003b). Regulation of phyllotaxis by polar auxin transport. *Nature* **426**, 255-260.

Resino, J., Salama-Cohen, P. and Garcia-Bellido, A. (2002). Determining the role of patterned cell proliferation in the shape and size of the Drosophila wing. *Proc. Natl. Acad. Sci. USA* **99**, 7502-7507.

Rolland-Lagan, A. G., Bangham, J. A. and Coen, E. (2003). Growth dynamics underlying petal shape and asymmetry. *Nature* **422**, 161-163.

Schoof, H., Lenhard, M., Haecker, A., Mayer, K. F., Jurgens, G. and Laux, T. (2000). The stem cell population of Arabidopsis shoot meristems in maintained by a regulatory loop between the CLAVATA and WUSCHEL genes. *Cell* **100**, 635-644.

Shapiro, B. E., Levchenko, A., Meyerowitz, E. M., Wold, B. J. and Mjolsness, E. D. (2003). Cellerator: extending a computer algebra system to include biochemical arrows for signal transduction simulations. *Bioinformatics* **19**, 677-678.

Smyth, D. R., Bowman, J. L. and Meyerowitz, E. M. (1990). Early flower development in Arabidopsis. *Plant Cell* **2**, 755-767.

Soma, K. and Ball, E. (1964). Studies of the surface growth of the shoot apex of Lupinus albus. *Brookhaven Symp. Biol*. **16**, 13-45.

Steeves, T. A. and Sussex, I. M. (1989). *Patterns in Plant Development: Shoot Apical Meristem Mutants of* Arabidopsis thaliana. New York: Cambridge University Press.

Wyrzykowska, J. and Fleming, A. (2003). Cell division pattern influences gene expression in the shoot apical meristem. *Proc. Natl. Acad. Sci. USA* **100**, 5561-5566.